metals

MDPI

Article

Effect of Thiourea on Lead Release from Lead-Bearing Jarosite under Freeze–Thaw Cycling

Jun Peng [1,2], Hui Liu [1,3,*], Yujun Shen [2], Luhua He [2], Yangjin Wei [1] and Xu Yan [1,3,*]

[1] School of Metallurgy and Environment, Central South University, Changsha 410083, China; pengjun@minmetals.com (J.P.); weiyangjin@csu.edu.cn (Y.W.)
[2] Changsha Research Institute of Mining and Metallurgy Co., Ltd., Changsha 410012, China; shenyujun@minmetals.com (Y.S.); heluhua@minmetals.com (L.H.)
[3] Chinese National Engineering Research Center for Control & Treatment of Heavy Metal Pollution, Changsha 410083, China
* Correspondence: leolau@csu.edu.cn (H.L.); yanxu1202@csu.edu.cn (X.Y.); Tel.: +86-731-88830875 (H.L. & X.Y.)

Abstract: Lead is a toxic factor in jarosite residue, and it is important to study its release behavior from simulated lead jarosite residue (LSJ) to predict the stability of the jarosite residue and its impact on the environment. This study investigated the ion release behavior, leaching toxicity, stability, and ion migration of LSJ during freeze–thaw cycling with thiourea (T-FTC). The release of lead, iron, and sulfate radicals from lead jarosite via T-FTC was influenced by several factors. Under specific conditions, the amount of lead released was 6.09 mM/L, which accounted for 38.3% of the total lead. After the T-FTC treatment, the residual lead increased, and the leaching toxicity and long-term stable equilibrium concentration of lead were reduced to 42.1 mg/L and 12.4 mg/L, respectively, which decreased by 82% and 84%, respectively and led to improved environmental stability. This study provides a novel approach for the safe disposal of jarosite residue under low-temperature and mild conditions, and the results can be used to predict the stability of jarosite residue and its secondary pollution in the environment.

Keywords: simulated lead-bearing jarosite; release behavior; freeze–thaw cycles; environmental stability; thiourea

check for updates

Citation: Peng, J.; Liu, H.; Shen, Y.; He, L.; Wei, Y.; Yan, X. Effect of Thiourea on Lead Release from Lead-Bearing Jarosite under Freeze–Thaw Cycling. *Metals* **2023**, *13*, 1053. https://doi.org/10.3390/met13061053

Academic Editor: Antoni Roca

Received: 15 May 2023
Revised: 29 May 2023
Accepted: 30 May 2023
Published: 31 May 2023

Copyright: © 2023 by the authors. Licensee MDPI, Basel, Switzerland. This article is an open access article distributed under the terms and conditions of the Creative Commons Attribution (CC BY) license (https://creativecommons.org/licenses/by/4.0/).

1. Introduction

The jarosite process is commonly utilized in hydrometallurgy for iron removal due to its ease of operation and slag filtration capabilities [1–3]. In China alone, it has been reported that more than 30 million tons of jarosite residue has been accumulated, with an increasing trend year by year, which poses a significant potential threat to the environment [4,5]. Some zinc hydrometallurgy plants store the jarosite residue in nearby construction slag yards, resulting in a large land footprint and significant environmental pollution risks [6,7]. Hage et al. [8] employed slag yard stockpiling to address the leakage issues of two jarosite residue ponds at the Budelco Zinc Plant in the Netherlands. Meanwhile, the other two slag ponds rely on deep-sea deposition and mountain landfills, which present severe environmental concerns. Between 1973 and 1997, Pasminco EZ Metals dealt with over 4 million tons of jarosite residue, and experienced lead and arsenic leaking, polluting the Tasmanian coast [9]. The landfilling of jarosite residue in granite caves in Oda, Norway, has resulted in lead leakage and contamination in the area [10]. Therefore, the safe disposal of jarosite residue poses a significant challenge.

Most studies of the heavy metals in jarosite residue have focused solely on coprecipitation behavior [11–16], while the release of heavy metals and the long-term stacking stability of jarosite residue remain unclear. Heavy metals such as Pb, Zn, Cd, and As in jarosite residue can continuously dissolve under natural conditions such as wind, sun, and rain, potentially polluting water and soil due to changes in external factors such as pH and

temperature [17–19]. This is particularly concerning since jarosite residue is considered hazardous waste in China and Europe [20,21]. Heavy metals are usually enriched in jarosite residue through coprecipitation or surface adsorption, which can affect their migration in the slag yard environment. As environmental conditions change, such as redox conditions, solution pH, temperature, and organic matter content, sodium jarosite in the slag will dissolve or phase transform, releasing toxic and harmful elements fixed on the surface or within the lattice [22]. Therefore, it is crucial to comprehend the rules governing the release and migration of heavy metals in jarosite residue yards, as well as devise methods for separating or solidifying heavy metals in jarosite residue.

Freeze–thaw cycling (FTC) is a gradual cyclic process of temperature change from low to high that occurs in the cold regions of the Earth. This phenomenon is quite common at middle and high latitudes and is the most typical climate feature in frozen soil and seasonally frozen soil areas [23–26]. FTC can have an impact on the physical and chemical properties of soil, slag, and other media, ultimately affecting the environmental behavior of heavy metals in those media [27,28]. Dang et al. [29] investigated the effect of FTC on the occurrence and migration of cadmium in unsaturated zone media and found that the frequency of FTC and water content can significantly affect the occurrence form of cadmium and promote its release in the medium. The macropores created by FTC can also increase the migration capacity of cadmium in the medium and elevate the risk of cadmium pollution in groundwater. Guo et al. [30] found that FTC can effectively reduce the adsorption of heavy metals in the medium, change the adsorption mechanism of heavy metals, and promote the desorption and release of heavy metals into the environment. Zhang et al. [31] studied the effect of FTC on the migration ability of cadmium and found that FTC could significantly increase the percentage of exchangeable cadmium in the medium, thereby enhancing the mobility of cadmium and promoting its movement to deeper soil. Meng et al. [32] found that FTC can age biochar in soil, increase its surface area, and significantly increase the content of fixed and migrated Cd. Wang et al. [33] found that FTC can increase the movable colloid of the soil, causing Pb to move deeper into the soil, and increasing the content of Pb in the soil depths.

Heavy metals exist in various chemical forms in the medium, which affects their mobility and bioavailability [34]. Wang et al. [35] observed that the exchangeable state of cadmium decreased while the bound state of iron and manganese oxides increased with the increasing moisture content caused by FTC. Li et al. [36] investigated the influence of dissolved organic matter on Pb in contaminated soil under FTC and found that Pb and organic matter can combine into a stable valence state, which can be extracted into a solution. It is speculated that heavy metal ions and organic matter are complexed and chelated in a covalent bond mode, thereby reducing the bioavailability and mobility of heavy metals and providing novel treatment strategies for contaminated soil. Moreover, FTC synergistic leaching is anticipated to enhance the leaching efficiency of heavy metals and thereby remediate heavy-metal-contaminated soils [37]. Rui et al. [38] used EDTA as the eluant and demonstrated the effective removal of Pb and Cd in cohesive soil after several freeze–thaw cycles. The removal rate of heavy metals increased with an increase in freeze–thaw and washing times. The destruction of the soil particle structure by FTC is believed to be the main reason for the improved removal rate, allowing the eluant to fully come into contact with the heavy metals in the soil and promoting the reaction between the eluant and heavy metals. These findings suggest that FTC with chemical reagents could be an effective approach for remediating heavy-metal-contaminated soil.

The differential FTC of solutes or minerals can be harnessed to achieve concentration and aggregation, thereby promoting chemical reactions, particularly those involving organic matter [39]. Thiourea, an organic compound with sulfur and amino groups, can form metal–thiourea complexes with lead, copper, zinc, silver, and other metals, albeit with slow reaction rates [40]. Previous studies by domestic and foreign scholars have explored the impact of FTC on the heavy metal behavior in soil, including on the adsorption and desorption behavior, occurrence state, bioavailability, migration and release, and form

transformation of heavy metals such as lead and cadmium, and analyzed the associated mechanisms in conjunction with soil physical and chemical parameters. Alternatively, thus far, there have been no studies conducted on the behavior of heavy metals in jarosite residue during the FTC process apart from those carried out by our team.

However, there are many impurities and complex structures in jarosite residue which are not conducive to the analysis of the migration law and environmental behavior of heavy metals in the jarosite residue. The previous research shows that the most important factor affecting the environmental stability of jarosite residue is lead [41,42]. Therefore, it is of great significance to study the release behavior of lead from simulated leached jarosite residue.

2. Materials and Methods

2.1. Materials

The chemicals used in this study were purchased from a reputable supplier (Sinopharm Chemical Reagent Co., Ltd., Beijing, China) and were of analytical reagent grade. The chemicals included ferric sulfate ($Fe_2(SO_4)_3 \cdot xH_2O$), sodium sulfate (Na_2SO_4), lead acetate ($Pb(CH_3COO)_2$), sodium hydroxide (NaOH), sulfuric acid (H_2SO_4), and thiourea ($(NH_2)_2CS$). All solutions were prepared using ultrapure water with a resistivity of 18 MΩ·cm. The contents of Fe, Pb, Na, and S in the simulated lead-bearing jarosite were 27.7%, 9.86%, 2.98%, and 14.2%, respectively.

2.2. Synthesis of Simulated Lead-Bearing Jarosite

The lead-bearing jarosite (LBJ) was synthesized in a 1 L solution by adding 0.25 mol/L $Fe_2(SO_4)_3 \cdot xH_2O$ and 0.06 mol/L Na_2SO_4, and by stirring constantly at 600 r/min at 95 °C. The pH was adjusted to 1.0 using a 7.0 mol/L NaOH solution, and then 100 mL of 0.3 mol/L $Pb(CH_3COO)_2$ solution was gradually added at a rate of 50 mL/h while stirring. To maintain the pH at 2.0, a NaOH solution was added during the reaction. After stirring the precipitates for 3 h, the residual supernatant solutions were settled and decanted. Following synthesis, the simulated jarosite was filtered using a vacuum, and then washed several times with ultrapure water (18 MΩ·cm) before being dried at 80 °C for 24 h [41].

2.3. Procedure of T-FTC

Thiourea stock solution was prepared and diluted to concentrations of 0, 0.05 M, 0.20 M, 0.40 M, 0.60 M, and 0.80 M (M: mol/L) for the experiment. The pH values of the thiourea solutions were adjusted to 1, 3, 6, 8, and 10 with H_2SO_4 or NaOH. For the pH 6 system, no buffer solution was added, as the pH value of the LBJ changed only slightly during the reaction. However, for the other pH conditions, a 0.05 mol/L MES (2-(N-Morpholino) ethanesulfonic acid) buffer solution, pre-adjusted to the specified pH value with sulfuric acid and sodium hydroxide, was added. Additionally, 1.00 g of LBJ was added to a series of 50 mL polyethylene centrifuge tubes, which was followed by the addition of 30 mL of thiourea solution. The tubes were shaken well and then placed on an ultrasonic washing machine for 2 min to mix the suspension thoroughly. The tubes were then placed in a centrifuge tube rack and stored in an ultra-low-temperature refrigerator (−20 °C) for 12 h to freeze the suspension. After freezing, the tubes were placed in a thermostatic water bath at 20 °C for 12 h to thaw. This process was repeated for 1, 3, 6, 9, and 12 freeze–thaw cycles (T-FTC). A control sample (CS) was also set up and kept in a constant-temperature water bath at 20 °C for heat preservation. After the reaction, the suspension was filtered through a 0.45 μm microporous membrane, and the filtrate was sampled for analysis of Pb, Fe, and SO_4^{2-}. The filter cake was washed with ultrapure water (18 MΩ/cm) and then dried in a freeze-drying oven for solid phase analysis.

2.4. Sequential Extraction Scheme

The Community Bureau of Reference (BCR) previously introduced a three-step extraction procedure to analyze heavy metal combination forms. In this study, the Davidson's three-stage BCR sequential extraction procedure was utilized to investigate the effective combination forms of heavy metals in the jarosite residue. The detailed procedures of the BCR tests can be found in previous studies [43,44].

2.5. Toxicity Characteristic Leaching Procedure

The Toxicity Characteristic Leaching Procedure (TCLP) is a well-established method recommended by the US Environmental Protection Agency (EPA) for evaluating the potential environmental risk of solid waste samples and determining whether they should be classified as hazardous waste or not. The TCLP method involves an extraction procedure that aims to simulate the leaching of metals (and organic compounds) from solid waste under acidic rainfall conditions. The detailed TCLP test procedure can be found in the literature [42,44].

2.6. Analysis

2.6.1. Determination of Elemental Composition

The concentrations of Pb and low-level Fe in the solution were analyzed using atomic absorption fluorescence spectrometry, while high-level Fe was determined through phenanthroline spectrophotometry [45]. Barium sulfate turbidimetry and ion chromatography were used to analyze the concentrations of high- and low-level SO_4^{2-}, respectively. The thiourea concentration was determined through mercury nitrate titration [46].

2.6.2. Other Analyses

The microstructure, surface morphology, and special chemical composition were observed using a scanning electron microscope (JEOL, Tokyo, Japan, JSM-7900F). The mineralogical composition of the samples was determined firstly by X-ray diffraction analysis (BRUKER, Karlsruhe, Germany, D8 ADVANCE) using Cu Kα radiation with steps of 0.02° at 10°/min in a 2θ range from 5° to 80° under operating conditions of 40 kV and 40 mA.

3. Results and Discussion

3.1. Effect of Thiourea on Release of Lead, Iron, and Sulfate under Freeze–Thaw Condition

3.1.1. Effect of Solution pH

The immobilization conditions were as follows: In total, 1 g of LBJ was subjected to immobilization with a thiourea concentration of 800 mM/L (millimoles per liter) and a liquid–solid ratio of 30 mL/g. The freezing temperature was set at −20 °C. The results are presented in Figure 1. The concentration of Pb in the solution phase initially increases and then decreases with the initial pH value, while the concentration of Fe decreases gradually and then stabilizes with the increase in pH value. As the number of freeze–thaw cycles increases, the release of Pb increases, while the release of Fe first increases and then slightly decreases, suggesting that freeze–thaw cycles can promote the release of Pb and Fe.

At a pH of 6 and 12 in T-FTC, the amount of Pb released from the solution is 6.09 mM/L, accounting for 38.3% of the total Pb. In contrast, the amount of Pb released from the solution is only 0.77 mM/L (4.87% of the total Pb content) in the control experiment corresponding to CS. These findings indicate that T-FTC can promote the reaction of Pb with thiourea and accelerate its release into the solution. When the pH is greater than 6, the release of Fe is only about 0.50 mM/L because at higher pH values, the Fe in the solution forms a ferric hydroxide precipitate, which readily adsorbs Pb in the solution and leads to a significant decrease in the release of Pb.

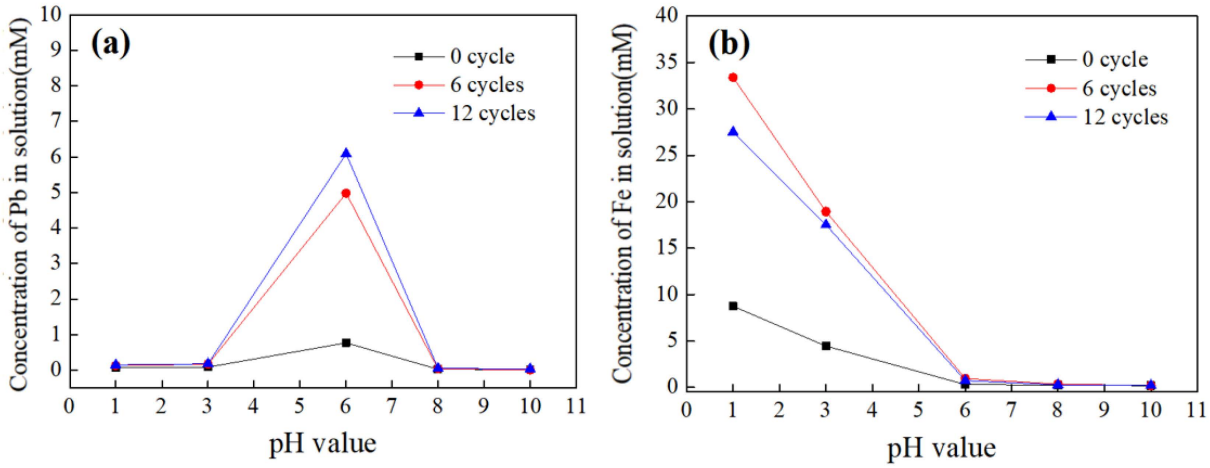


Figure 1. Ion concentration in solution varied with pH value after T-FTC of LBJ. (**a**) Pb; (**b**) Fe.

At a pH of 1, the release amount of Fe is relatively high. For T-FTC with 0, 6, and 12 cycles, the total release amount of Fe is 8.75 mM/L, 33.4 mM/L, and 27.5 mM/L, respectively, accounting for 5.30%, 20.3%, and 16.7% of the total Fe content in the reaction system. This observation may be due to the instability of the jarosite phase at pH 1 and 3, making it prone to decomposition and dissolution, and resulting in an increase in the release of Fe. In contrast, lead does not participate in the dissolution reaction of dilute sulfuric acid, resulting in a low lead content in the solution.

To further understand the effect of the pH value in the T-FTC process on the phase and micromorphology of LBJ, XRD and SEM-EDS analyses were conducted for 12 T-FTC cycles under different pH values (3, 6, 8, and 10). The results are presented in Figures 2 and 3.

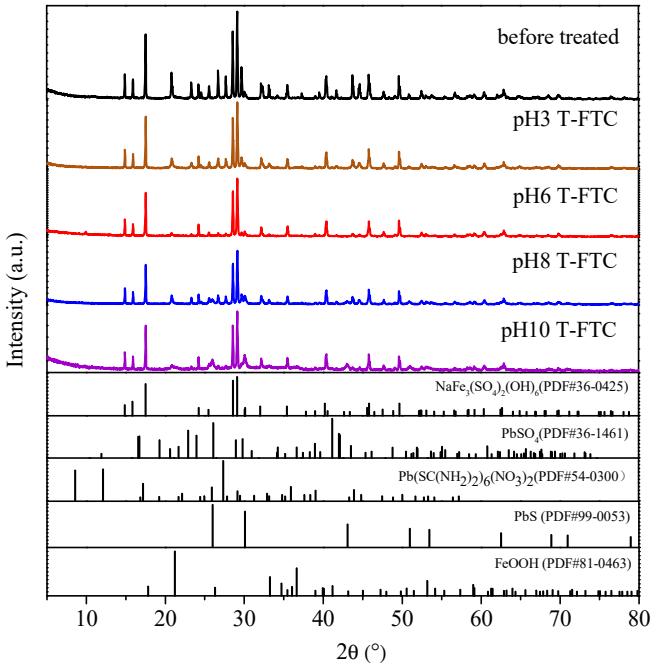


Figure 2. XRD patterns of LBJ using 12 T-FTC cycles with different pH values (before treated means LBJ without any treatment).

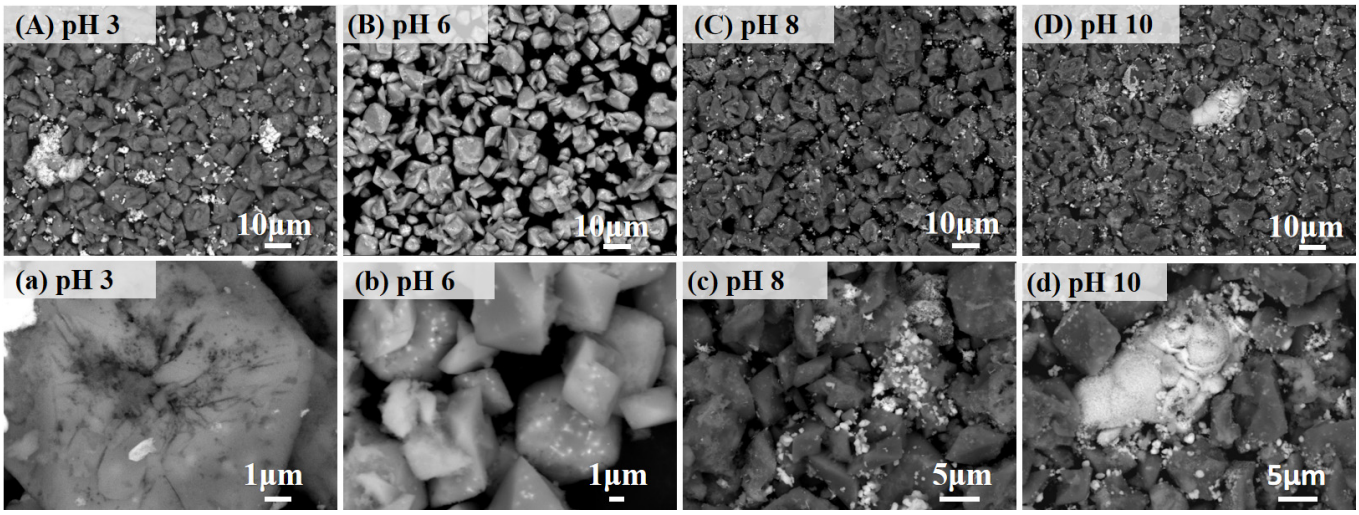


Figure 3. SEM images of LBJ using 12 T-FTC cycles with different pH values. (**A**,**a**) pH 3; (**B**,**b**) pH 6; (**C**,**c**) pH 8; (**D**,**d**) pH 10.

The results indicate that at pH 3, the jarosite crystals treated by T-FTC are corroded by acid (Figure 3a), leading to the formation of numerous pits and grooves on the previously smooth and compact surface, and resulting in a fluffy jarosite matrix. This structure is conducive to the adsorption of dissolved Pb ions or Pb-tu generated by the reaction, resulting in a low lead content in the solution. At pH 6, the lead sulfate embedded on the surface of the lead-containing jarosite treated by T-FTC has mostly fallen off (Figure 3b). The crystal structure of jarosite remains essentially unchanged, and XRD analysis (Figure 2) shows that the characteristic diffraction peak of lead sulfate decreases compared with that of lead-containing jarosite before being treated. It is possible that thiourea can decompose into S^{2-} at a high pH and form a PbS precipitate, which appears as submicron floc on the surface of the jarosite matrix in SEM analysis. Alternatively, the increase in pH can cause the secondary hydrolysis of iron in the solution to form flocculent ferric hydroxide. At pH 10, more flocculent precipitates are distributed on the surface of the jarosite, as shown in Figure 3d. Furthermore, a bright white film, which is different from the fine particles, encases the jarosite. XRD analysis reveals the presence of a new phase of PbS, which is presumed to be a layer of wrapping film formed by submicron PbS particles gathering near the goethite.

3.1.2. Effect of Thiourea Concentration

Experimental conditions: In total, 1 g of LBJ was used with a liquid–solid ratio of 30 mL/g and a freezing temperature of −20 °C. The release of the Pb and Fe in the LBJ into the solution was investigated under the conditions of a thiourea concentration of 0 mM/L, 200 mM/L, 400 mM/L, 600 mM/L, and 800 mM/L; pH values of 3 and 6; and T-FTC with 0 and 6 cycles. The results are shown in Figure 4.

The results show that T-FTC had little effect on the release of Pb at pH 3, and the amount of Pb released is less than 0.2 mM/L (1.20% of total Pb), while the amount of Fe released increased with the increase in thiourea concentration. As the thiourea concentration increased from 200 mM/L to 600 mM/L, the amount of released Fe increased from 1.63 mM/L (0.99% of total Fe) to 18.93 mM/L (11.5% of total Fe). These results indicate that T-FTC accelerated the reaction between thiourea and jarosite under acidic conditions, and the reaction intensified with the increase in thiourea concentration.

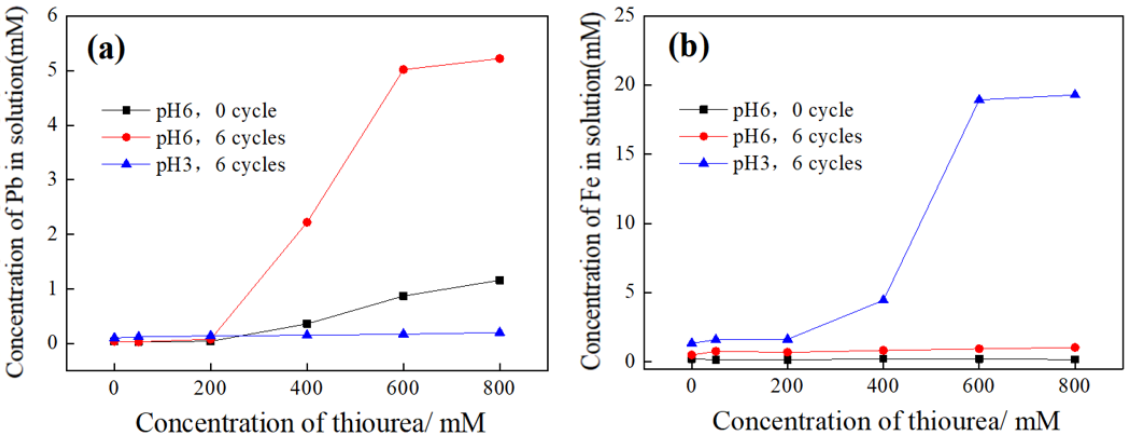


Figure 4. Ion concentration in solution varied with thiourea concentration after T-FTC of LBJ. (**a**) Pb; (**b**) Fe.

At pH 6, the amount of Pb and Fe released in the CS without T-FTC is minimal. However, after 6 cycles of T-FTC treatment, the amount of Pb released significantly increases with the rise in the thiourea concentration. At a thiourea concentration of 800 mM/L, the amount of Pb released is 5.22 mM/L, accounting for 32.9% of the total Pb, and indicating that T-FTC can promote the reaction between thiourea and lead. The amount of Fe released is low, less than 1 mM/L, indicating that T-FTC had no effect on the release of Fe at pH 6, which provides favorable conditions for the subsequent separation of Pb and Fe.

3.1.3. Effect of Freeze–Thaw Cycles

The experimental conditions were as follows: In total, 1 g of LBJ was treated with a thiourea concentration of 800 mM/L and a liquid–solid ratio of 30 mL/g, and was frozen at −20 °C. The release of Pb and Fe from the LBJ into the solution was investigated at different T-FTC cycles (1, 3, 6, 9, and 12) and pH values (3 and 6). The results shown in Figure 5 indicate that T-FTC had no effect on the release of Pb at pH 3, which remains below 0.2 mM/L. The release of Fe decreased slightly with increasing T-FTC cycles, suggesting that its release could be inhibited by increasing the number of T-FTC cycles. The release of Pb increases with an increase in freeze–thaw cycles at pH 6. As the number of cycles increases from 1 to 12, the release of Pb increases from 2.22 mM/L (14.0% of total Pb) to 6.09 mM/L (38.3% of total Pb). Thus, increasing the number of freeze–thaw cycles is found to be beneficial for the release of Pb, while the release of Fe stayed below 1 mM/L.

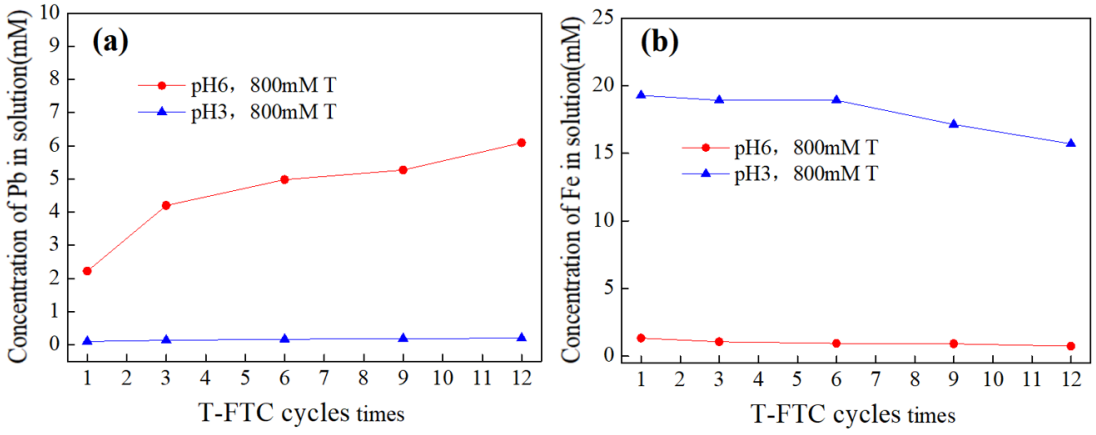


Figure 5. Ion concentration in solution varied with T-FTC cycle times after T-FTC of LBJ. (**a**) Pb; (**b**) Fe.

3.1.4. Effect of Freezing Temperature

The experimental conditions included 1 g of LBJ, a thiourea concentration of 800 mM/L, a liquid–solid ratio of 30 mL/g, a pH value of 6, and 6 freeze–thaw cycles to study the release of lead, iron, and sulfate ions from the LBJ into the solution at freezing temperatures ranging from −5 °C to −50 °C. The results presented in Figure 6 show that the release of Fe remains almost constant at pH 6 as the freezing temperature increases, remaining below 1 mM/L (0.6% of total Fe). The release of Pb increases initially, then decreases, and increases again as the freezing temperature increases. Low or high freezing temperatures are not favorable for the release of Pb, with the optimal release occurring at temperatures lower than −20 °C. The release behavior of SO_4^{2-} and Pb is similar, indicating that the release of SO_4^{2-} is mainly due to the release of $PbSO_4$ by the reaction of thiourea with lead.

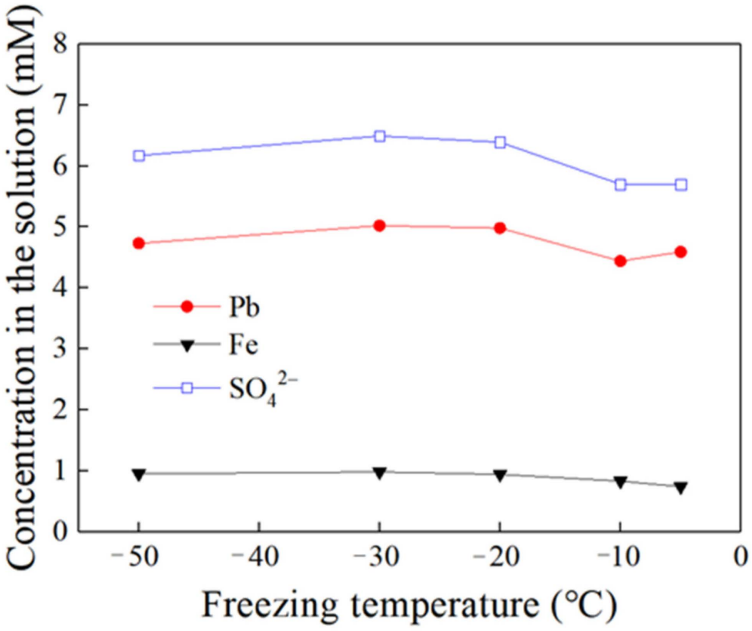


Figure 6. Ion concentration in solution with various freezing temperatures after T-FTC of LBJ.

3.1.5. Effect of Freeze–Thaw Methods

The experimental conditions were as follows: In total, 1 g of LBJ, a thiourea concentration of 800 mM/L, a liquid–solid ratio of 30 mL/g, a pH of 6, and 6 T-FTC cycles. Different freeze–thaw methods (A: frozen at −20 °C for 12 h and thawed at 20 °C for 12 h; B: frozen in liquid nitrogen for 5 min and thawed at 20 °C for 12 h; C: frozen in liquid nitrogen for 5 min and thawed at 20 °C for 6 h; and D: frozen in liquid nitrogen for 5 min and thawed in a microwave for 5 min) were investigated to determine their effect on the release of lead, iron, and sulfate ions from LBJ. The results presented in Figure 7 demonstrate that the release of Pb and SO_4^{2-} was reduced to a certain extent after rapid freezing using liquid nitrogen under the B mode. Specifically, the concentration of Pb in the solution decreased from 5.02 mM/L (31.64% of total Pb) to 2.56 mM/L (16.13% of total Pb), while the concentration of SO_4^{2-} also decreased from 6.44 mM/L (4.92% of total) to 3.70 mM/L (2.83% of total). In contrast, altering the thawing method (C and D) by using ultrasonic or microwave rapid thawing was found to inhibit the release of Pb, Fe, and SO_4^{2-}. Moreover, the rate of ion release was inversely proportional to the speed of thawing. Notably, the release of Pb decreased to 1.01 mM/L (6.39%) with microwave rapid thawing, indicating that this thawing method is unsuitable for the present purposes.

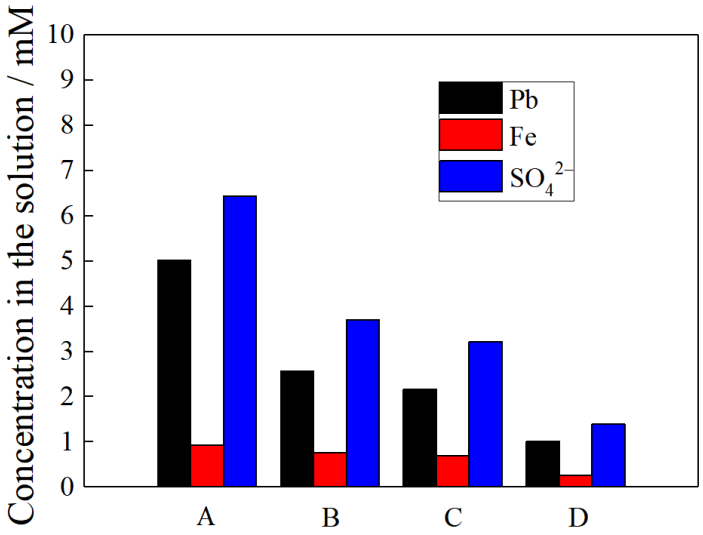


Figure 7. Ion concentration in solution with various freeze–thaw methods after T-FTC of LBJ. (A: frozen at −20 °C for 12 h, thawed at 20 °C for 12 h; B: frozen in liquid nitrogen for 5 min, thawed at 20 °C for 12 h; C: frozen in liquid nitrogen for 5 min, thawed at 20 °C for 6 h; D: frozen in liquid nitrogen for 5 min, thawed in microwave for 5 min).

3.2. Effect of Thiourea Freeze–Thaw Cycles on the Speciation of Lead

Figure 8 displays the lead transformation in LBJ under various freeze–thaw treatments. BT refers to the LBJ before treatment, FTC indicates a sample subjected to a blank freeze–thaw cycle without thiourea, and T-FTC refers to a sample treated with 800 mM/L of thiourea using T-FTC. The other freeze–thaw conditions included a liquid–solid ratio of 30 mL/g, a freezing temperature of −20 °C, a pH value of 6, and 12 freeze–thaw cycles. The YD-T-FTC sample was quickly frozen for 5 min using liquid nitrogen, with the other conditions the same as those of the T-FTC sample.

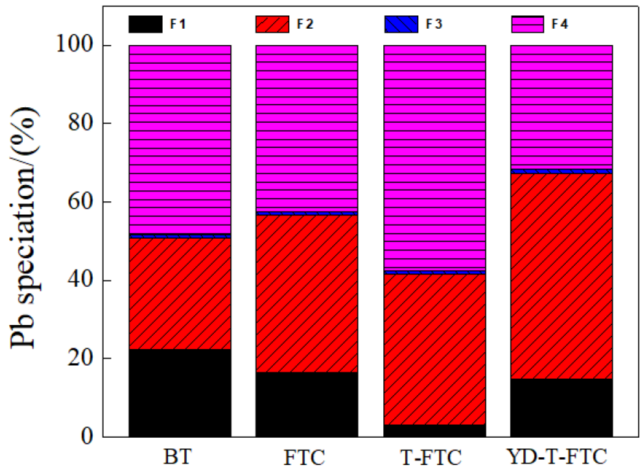


Figure 8. Effects of different treatment conditions on the form of lead in LBJ (F1: exchangeable Pb; F2: reducible Pb; F3: oxidizable Pb; F4: residual Pb).

The results indicate that the distribution of lead in different fractions varied significantly. The ratios of F1, F2, F3, and F4 lead to the total lead of LBJ are 22.32%, 28.40%, 0.90%, and 48.28%, respectively. After undergoing FTC treatment, there is a slight decrease in F1, while the content of F2 increases significantly. However, there is only a minor change in F3, and a slight decrease is observed in F4. The corresponding ratios of F1, F2, F3, and F4 are 16.4%, 40.3%, 0.78%, and 42.5%, respectively. In contrast, the contents of F1, F2, F3, and

F4 are 3.01%, 38.6%, 0.73%, and 57.6%, respectively, after T-FTC treatment. This indicates a significant decrease in the proportion of exchangeable lead, with a minor decrease in the proportion of reducible lead. Additionally, the proportions of oxidizable and residual lead increase, signifying an improvement in the environmental stability of LBJ after T-FTC treatment. Further, the proportions of F1, F2, F3, and F4 are 14.85%, 52.44%, 0.97%, and 31.74%, respectively, after YD-T-FTC treatment. In comparison with T-FTC, there is a slight decrease in exchangeable lead content, while the content of reducible lead increases significantly, and residual lead decreases. These results suggest that rapid freezing is not beneficial for the detoxification of LBJ, and environmental stability decreases as a result.

3.3. Ion Migration Changes in T-FTC Process of Lead Jarosite

Table 1 displays the changes in the ion migration of LBJ during the T-FTC process. The results show that the concentration of lead and thiourea in the unfrozen solution is around nine and three times higher than that in the icicle, respectively. The proportion of Pb released by LBJ through T-FTC in the unfrozen solution and icicle is 23.2% and 15.7%, respectively. In the lower part of the icicle, the concentrations of lead and thiourea are 24% and 48% higher than those in the upper part, respectively, while in the unfrozen solution, the concentration of lead and thiourea in the lower part is only 2% and 8% higher than that in the upper part. The ion transfer between the ice column and the unfrozen solution is similar, and the concentration of ions in the lower part is higher than that in the upper part. The phenomenon of ion enrichment in the unfrozen solution is consistent with the concentration and aggregation in the freeze–thaw solution, indicating that freeze–thaw cycling promotes the movement of ions to the unfrozen solution. Once thiourea reaches a certain concentration in the unfrozen solution, it can accelerate the reaction between thiourea and lead in jarosite, and hence, release lead at a faster rate.

Table 1. Experimental results of ion migration in T-FTC process.

Items		Volume (mL)	Concentration (g/L)		Percentage (%)	
			Pb	tu	Pb	tu
Icicle	upper part	13.2	0.53	36.6	7.10	26.5
	lower part	12.8	0.66	54.2	8.57	38.0
Unfrozen Solution	upper part	2.20	4.81	120	10.7	14.5
	lower part	2.50	4.92	130	12.5	17.8

3.4. Environmental Stability

A leaching toxicity test was conducted on the LBJ following treatment with T-FTC (800 mM/L of thiourea, pH 6, and 12 freeze–thaw cycles). Table 2 compares the leaching toxicity of LBJ before and after the T-FTC treatment. The results demonstrate that the leaching toxicity of lead in the TLPC methods was reduced to 42.2 mg/L after treatment by T-FTC. This represents an approximately 82% reduction in leaching toxicity compared to that before the treatment, indicating that the T-FTC treatment effectively reduces the leaching toxicity of lead in jarosite residue.

Table 2. The leaching toxicity of Pb from LBJ before and after T-FTC.

Element	Identification Standards for Hazardous Waste/(mg·L^{-1})	Leaching Toxicity before Treatment/(mg·L^{-1})	Leaching Toxicity after T-FTC/(mg·L^{-1})
Pb	5	238	42.1

Table 3 shows the results of the environmental stability test conducted on LBJ after treatment with T-FTC (800 mM/L of thiourea, pH 6, and 12 T-FTC cycles). The data suggest that the concentration of Pb in the leaching solution of LBJ after T-FTC treatment was significantly lower than that before the treatment, as reported in reference [36]. During the initial 48 h of continuous leaching, the concentration of Pb in the leaching solution was relatively high, ranging from 38 to 42 mg/L. After continuous leaching for 168 h, the concentration of Pb decreased to 18 mg/L, and thereafter remained between 11 and 14 mg/L. The reaction reached equilibrium, with an equilibrium concentration of Pb of about 12 mg/L, compared to an equilibrium concentration of Pb of 75 mg/L before the treatment. The toxic release concentration of Pb after the T-FTC treatment decreased by 84%, and the environmental stability was significantly improved. However, the leaching toxicity of Pb still exceeded the identification standard of Pb toxicity (5 mg/L). Increasing the number of freeze–thaw cycles, applying external fields (such as ultrasound or mechanical activation) in conjunction with freeze–thaw cycling, or solidifying lead in a stable state using solidifying agents such as phosphate may further reduce the leaching toxicity of Pb.

Table 3. Variation in leaching concentration of Pb with time in the continuous leaching experiment of LBJ.

No.	Time (h)	Concentration of Lead in Solution (mg/L)	η_{Pb} * (%)
1	24	41.6	0.07
2	48	38.7	0.20
3	72	29.9	0.35
4	96	28.7	0.54
5	120	26.3	0.75
6	144	21.4	0.97
7	168	18.6	1.18
8	192	14.3	1.37
9	216	12.9	1.57
10	240	13.1	1.78
11	264	14.1	2.04
12	288	13.2	2.30
13	312	12.5	2.57
14	336	12.4	2.86
15	360	12.5	3.17
16	384	11.8	3.48
17	432	12.7	3.86
18	456	12.8	4.27
19	480	12.4	4.68

* η_{Pb} means the proportion of the total accumulated leaching amount in relation to the total lead.

4. Conclusions

This paper investigated the effects of thiourea on the release, migration, and environmental stability of lead in synthetic simulated jarosite residue (LBJ) under freeze–thaw conditions. Factors influencing lead release include pH value, thiourea concentration, number of freeze–thaw cycles, freeze temperature, and freeze–thaw mode. The release of lead initially increases and then decreases with an increase in the pH value and increases with an increase in thiourea concentration and number of freeze–thaw cycles. Freezing temperatures that are too low or too high, and rapid freeze–thaw cycles, are not favorable for lead release, and the suitable freezing temperature range is from -20 °C to -40 °C. Iron is released at low pH values (pH $\leq$ 3) but not at high pH values (pH $\geq$ 6), and sulfate release is consistent with that of lead.

Under optimized conditions (thiourea concentration of 200 mM/L, pH 6, -20 °C freezing, and 12 T-FTC cycles), 6.09 mM/L of lead was released, accounting for 38.34% of the total lead, and iron was not released. The T-FTC treatment decreased the amount of

exchangeable lead significantly, while the amount of reduced lead decreased slightly, and the amount of oxidized and residual lead increased, leading to improved environmental stability. The lead leaching toxicity was reduced by 82% (the final concentration of lead was 42.1 mg/L), and the equilibrium concentration of lead in the long-term stable leaching solution was reduced by 84% (the final equilibrium concentration of lead was 12.4 mg/L), significantly improving environmental stability.

Author Contributions: J.P., H.L. and X.Y. conceived and designed the experiments; J.P., Y.W. and L.H. analyzed the data; J.P. wrote and edited the paper; X.Y., H.L. and Y.S. revised the work critically for important intellectual content. Conceptualization: J.P. and Y.S.; methodology: J.P., L.H. and Y.W.; software: J.P., Y.W. and L.H.; validation: J.P., Y.W. and Y.S. All authors have read and agreed to the published version of the manuscript.

Funding: This work was supported by the Major Program Natural Science Foundation of the Hunan Province of China (No. 2021JC0001), the National Natural Science Foundation of China (No. 22276218), and the National Key R and D Program of China (No. 2021YFC2902804).

Data Availability Statement: The data used in this study cannot be publicly released due to privacy and ethical concerns, as well as ongoing funding projects. However, we assure readers that our conclusions were reached through rigorous analysis and methodologies. We will consider sharing the data once all funding projects are complete and privacy/ethical issues are addressed.

Acknowledgments: We gratefully acknowledge the many important contributions from the researchers of all the reports cited in our paper.

Conflicts of Interest: The authors declare no conflict of interest.

References

1. Kushwaha, P.; Agarwal, M.; Ghosh, A. Value-added products from jarosite hazardous waste: A review. *Mater. Today Proc.* **2022**, *76*, 201–205. [CrossRef]
2. Eftekhari, N.; Kargar, M.; Rokhbakhsh Zamin, F.; Rastakhiz, N.; Manafi, Z. A review on various aspects of jarosite and its utilization potentials. *Ann. Chim.-Sci. Mater.* **2020**, *44*, 43–52. [CrossRef]
3. Asimi, A.; Gharibi, K.; Abkhoshk, E.; Moosakazemi, F.; Chelgani, S.C. Effects of Operational Parameters on the Low Contaminant Jarosite Precipitation Process-an Industrial Scale Study. *Materials* **2020**, *13*, 4662. [CrossRef]
4. Wang, Y.; Yang, H.; Zhang, G.; Kang, J.; Wang, C. Comprehensive recovery and recycle of jarosite residues from zinc hydrometallurgy. *Chem. Eng. J. Adv.* **2020**, *3*, 100023. [CrossRef]
5. Ge, H.; Pan, Z.; Xie, F.; Lu, D.; Wang, W.; Wu, S. Recovery of Valuable Metals by Roasting of Jarosite in Cement Kiln. *Metals* **2023**, *13*, 250. [CrossRef]
6. Parbhakar-Fox, A.; Gilmour, S.; Fox, N.; Olin, P. Geometallurgical characterization of non-ferrous historical slag in western Tasmania: Identifying reprocessing options. *Minerals* **2019**, *9*, 415. [CrossRef]
7. Li, L.; Tian, S.; Li, Y.; Li, J.; Huang, J.; Hu, X. Study on the Role of Quartz in the Bio-Oxidation of Sulfide Minerals from Mine Solid Waste. *Bull. Environ. Contam. Toxicol.* **2021**, *107*, 1103–1110. [CrossRef]
8. Hage, J.T.L.; Schuiling, R.D. Comparative column elution of jarosite waste and its autoclaved product-evidence for the immobilization of deleterious elements in jarosite. *Miner. Eng.* **2000**, *13*, 287–296. [CrossRef]
9. Gwyther, D. Impact of the deposition of jarosite on deepwater meiobenthos in southeastern Australia. *Mar. Pollut. Bull.* **2004**, *48*, 997–1003. [CrossRef]
10. Smeaton, C. Investigating the Susceptibility of Jarosite Minerals to Reduce Dissolution by a Dissimilatory Metal Reducing Bacterium. Ph.D. Thesis, University of Windsor, Windsor, ON, Canada, 2012.
11. Dutrizac, J.E.; Kaiman, S. Synthesis and properties of jarosite-type compounds. *Can. Mineral.* **1976**, *14*, 151–158.
12. Dutrizac, J.E. Factors affecting alkali jarosite precipitation. *Metall. Trans. B* **1983**, *14*, 531–539. [CrossRef]
13. Ripmeester, J.A.; Ratcliffe, C.I.; Dutrizac, J.E.; Jambor, J.L. Hydronium ion in the alunite-jarosite group. *Can. Mineral.* **1986**, *24*, 435–447.
14. Viñals, J.; Nunez, C.; Carrasco, J. Leaching of gold, silver and lead from plumbojarosite-containing hematite tailings in HCl $CaCl_2$ media. *Hydrometallurgy* **1991**, *26*, 179–199. [CrossRef]
15. Smith, A.M.; Dubbin, W.E.; Wright, K.; Hudson-Edwards, K.A. Dissolution of lead-and lead-arsenic-jarosites at pH 2 and 8 and 20 °C: Insights from batch experiments. *Chem. Geol.* **2006**, *229*, 344–361. [CrossRef]
16. Reyes, I.A.; Patiño, F.; Flores, M.U.; Pandiyan, T.; Cruz, R.; Gutiérrez, E.J.; Flores, V.H. Dissolution rates of jarosite-type compounds in H_2SO_4 medium: A kinetic analysis and its importance on the recovery of metal values from hydrometallurgical wastes. *Hydrometallurgy* **2017**, *167*, 16–29. [CrossRef]

17. Nolasco, M.C.; Flores, L.F.; Gutiérrez, E.J.; Aguilar, J.; Palacios, E.G.; Flores, M.U.; Reyes, I.A. Acid dissolution of jarosite-type compounds: Effect of the incorporation of divalent cations into the structure on the reaction rate. *Hydrometallurgy* **2022**, *212*, 105907. [CrossRef]
18. Hoeber, L.; Steinlechner, S. A comprehensive review of processing strategies for iron precipitation residues from zinc hydrometallurgy. *Clean. Eng. Technol.* **2021**, *4*, 100214. [CrossRef]
19. Wang, R.; Yan, Q.; Su, P.; Shu, J.; Chen, M.; Xiao, Z.; Cheng, Z. Metal mobility and toxicity of zinc hydrometallurgical residues. *Process Saf. Environ. Prot.* **2020**, *144*, 366–371. [CrossRef]
20. Song, X.; Ali, M.; Zhang, X.; Sun, H.; Wei, F. Stakeholder coordination analysis in hazardous waste management: A case study in China. *J. Mater. Cycles Waste Manag.* **2021**, *23*, 1873–1892. [CrossRef]
21. Comel, J.; Meux, E.; Leclerc, N.; Diliberto, S.; Pierrat, P.; Muhr, H. Use of Phytic Acid for the Removal of Iron in Hot Acidic Leachate from Zinc Hydrometallurgy. *JOM* **2021**, *73*, 1652–1660. [CrossRef]
22. Trueman, A.M.; McLaughlin, M.J.; Mosley, L.M.; Fitzpatrick, R.W. Composition and dissolution kinetics of jarosite-rich segregations extracted from an acid sulfate soil with sulfuric material. *Chem. Geol.* **2020**, *543*, 119606. [CrossRef]
23. Gao, D.; Bai, E.; Yang, Y.; Zong, S.; Hagedorn, F. A global meta-analysis on freeze-thaw effects on soil carbon and phosphorus cycling. *Soil Biol. Biochem.* **2021**, *159*, 108283. [CrossRef]
24. Xu, G.; Zheng, Q.; Yang, X.; Yu, R.; Yu, Y. Freeze-thaw cycles promote vertical migration of metal oxide nanoparticles in soils. *Sci. Total Environ.* **2021**, *795*, 148894. [CrossRef]
25. Sun, B.; Ren, F.; Ding, W.; Zhang, G.; Huang, J.; Li, J.; Zhang, L. Effects of freeze-thaw on soil properties and water erosion. *Soil Water Res.* **2021**, *16*, 205–216. [CrossRef]
26. Zhao, D.; Zhu, Y.; Wu, S.; Lu, Q. Simulated response of soil organic carbon density to climate change in the Northern Tibet permafrost region. *Geoderma* **2022**, *405*, 115455. [CrossRef]
27. Rizwan, M.; Ali, S.; Adrees, M.; Rizvi, H.; Zia-ur-Rehman, M.; Hannan, F.; Ok, Y.S. Cadmium stress in rice: Toxic effects, tolerance mechanisms, and management: A critical review. *Environ. Sci. Pollut. Res.* **2016**, *23*, 17859–17879. [CrossRef]
28. Guo, P.; Song, Y.; Xie, L.; Zhang, X.; Li, M.; Zhang, S. Effects of Freezing and Thawing on Adsorption/Desorption Characteristics of Pb and Cd in Black Soil and Brown Soil. *J. Jilin Univ. Earth Sci. Ed. China* **2012**, *01*, 229–235.
29. Dang, X.; Zhang, Y.; Yu, N.; Zhang, Y.; Song, Y. Effects of freeze-thaw cycles on the speciation of Cd in soils. *Chin. J. Soil Sci.* **2008**, *39*, 826–830.
30. Guo, P.; Li, Y.; Zhang, Y.; Ming, L.; Zhang, S.; Li, Y. Effects of freeze-thaw cycles on heavy metal adsorption in soils. *J. Jilin Univ. Sci. Ed. China* **2012**, *50*, 593.
31. Zhang, S. Effects of Freeze-Thaw Cycles on Migration and Transformation of Cd in Black Soil of Typical Farmland in Northeast China. Master's Thesis, Jilin University, Changchun, China, 2014.
32. Meng, Z.; Huang, S.; Xu, T.; Deng, Y.; Lin, Z.; Wang, X. Transport and transformation of Cd between biochar and soil under combined dry-wet and freeze-thaw aging. *Environ. Pollut.* **2020**, *263*, 114449. [CrossRef]
33. Wang, Z.; Zou, H.; Fan, Q.; Cen, J.; Zhang, Y. Effects of freeze-thaw cycles on migration of colloids and colloidal-bound lead in soil. *J. Agro-Environ. Sci. China* **2019**, *38*, 342–347.
34. Adamo, P.; Denaix, L.; Terribile, F.; Zampella, M. Characterization of heavy metals in contaminated volcanic soils of the Solofrana river valley (southern Italy). *Geoderma* **2003**, *117*, 347–366. [CrossRef]
35. Wang, Y.; Liu, J.; Wang, G.; Wang, J. Effects of freezing-thawing frequency and moisture content on cadmium speciation in black soil. *Chin. J. Environ. Sci.* **2007**, *27*, 693–697.
36. Li, Y.; Kang, C.; Zhang, Y.; Ming, L.; Zhang, S.; Guo, P. Leaching behavior of heavy metal Pb in contaminated soil under freeze-thaw cycles influenced by dissolved organic matter. *J. Jilin Univ. Earth Sci. Ed. China* **2013**, *43*, 945–952.
37. Rui, D.H.; Wu, Z.P.; Wu, Y.F.; Chen, X.; Liu, J.F.; Ding, J. Synergistic remediation of Cd and Pb-contaminated sticky soil by freezing-thawing and chemical leaching method. *Trans. Chin. Soc. Agric. Eng.* **2018**, *34*, 199–205.
38. Rui, D.; Wu, W.; Zhang, H.; Li, G.; Wang, S.; Ito, Y. Optimization analysis of heavy metal pollutants removal from fine-grained soil by freeze-thaw and washing technology. *Cold Reg. Sci. Technol.* **2020**, *173*, 103025. [CrossRef]
39. Xiao, L.; Zhang, Y.; Li, P.; Xu, G.; Shi, P.; Zhang, Y. Effects of freeze-thaw cycles on aggregate-associated organic carbon and glomalin-related soil protein in natural-succession grassland and Chinese pine forest on the Loess Plateau. *Geoderma* **2019**, *334*, 1–8. [CrossRef]
40. Ilyas, S.; Munir, H.; Kim, H.; Srivastava, R.R. Urban Mining of Precious Metals with Thiosulfate and Thiourea as Lixiviant. In *Sustainable Urban Mining of Precious Metals*; CRC Press: Boca Raton, FL, USA, 2021; pp. 123–148.
41. Jun, P.; Wei, Y.J.; Shi, M.Q.; Wu, J.H.; Wang, Q.W.; Zhang, L.; Hui, L.; Xu, Y. Spontaneous separation of Pb from $PbSO_4$-coprecipitated jarosite using freeze-thaw cycling with thiourea. *Trans. Nonferrous Met. Soc. China* **2022**, *32*, 1019–1030.
42. Jun, P.; He, L.H.; Hui, L.; Sun, Z.M.; Xu, Y. The Synthesis of Lead-Bearing Jarosite and Its Occurrence Characteristic and Leaching Toxicity Evaluation. *Metals* **2023**, *13*, 941.
43. Pueyo, M.; Mateu, J.; Rigol, A.; Vidal, M.; López-Sánchez, J.F.; Rauret, G. Use of the modified BCR three-step sequential extraction procedure for the study of trace element dynamics in contaminated soils. *Environ. Pollut.* **2008**, *52*, 330–341. [CrossRef]
44. Min, X.B.; Xie, X.D.; Chai, L.Y.; Liang, Y.J.; Mi, L.I.; Yong, K.E. Environmental availability and ecological risk assessment of heavy metals in zinc leaching residue. *Trans. Nonferrous Met. Soc. China* **2013**, *23*, 208–218. [CrossRef]

45. Tamura, H.; Goto, K.; Yotsuyanagi, T.; Nagayama, M. Spectrophotometric determination of iron (II) with 1,10-phenanthroline in the presence of large amounts of iron (III). *Talanta* **1974**, *21*, 314–318. [CrossRef]
46. Gupta, P.C. Analytical chemistry of thiocarbamides: I. Quantitative determination of thiourea. *Fresenius' Z. Anal. Chem.* **1963**, *196*, 412–431. [CrossRef]

Disclaimer/Publisher's Note: The statements, opinions and data contained in all publications are solely those of the individual author(s) and contributor(s) and not of MDPI and/or the editor(s). MDPI and/or the editor(s) disclaim responsibility for any injury to people or property resulting from any ideas, methods, instructions or products referred to in the content.